

## Article

# Joint Scheduling and Power Allocation Using Non-Orthogonal Multiple Access in Multi-Cell Beamforming Networks

Kyungseop Shin <sup>1</sup>  and Ohyun Jo <sup>2,\*</sup> <sup>1</sup> Department of Computer Science, Sangmyung University, Seoul 03016, Korea; akacking@gmail.com<sup>2</sup> Department of Computer Science, Chungbuk National University, Cheongju 28644, Korea

\* Correspondence: ohyunjo@chungbuk.ac.kr; Tel.: +82-43-261-2328

Received: 12 April 2020; Accepted: 26 May 2020; Published: 28 May 2020



**Abstract:** The proliferation of smart devices has boosted the improvement of wireless network technologies. Herein, networking functions should be properly guaranteed even in highly dense environments in terms of service quality and data rate. In this paper, we present an efficient power allocation algorithm using non-orthogonal multiple access and smart array antennas to increase the capacity in highly overlapped multi-cell environments. We evaluate the proposed algorithm and compare with the conventional orthogonal multiple access scheme with smart antennas. Through intensive simulations and experiments at the system level for performance evaluations, it is confirmed that the proposed scheme obtains a drastic throughput gain up to 50% in the overlapped region of highly dense networks.

**Keywords:** multiple access interference; directional antennas; wireless LAN; resource management; interference

## 1. Introduction

NOMA (non-orthogonal multiple access) is a promising technology in view of throughput increase via using superposition coding of multiple users. Multiple users can be supported simultaneously [1,2]. On the other hand, a smart array antenna offers directionality of the channel, which enables additional gain and reduces interference by producing directional beams of the transmit signal [3–7]. In spite of the notable advancements of each area, the relatively high computational complexity and huge portion of overlapped region in dense networks remain problematic to apply them in practical systems. Moreover, for the dense networks in the real world, multiple numbers of beams in multi-cell environments should be taken into account in practice.

As an attempt to combine beamforming and NOMA, joint optimization of scheduling and power allocation was presented in single cell environments [8]. Downlink spatial inter-cell interference cancellation was considered to mitigate other cell interference in [9]. They simplified the beamforming algorithm to mitigate spatial inter-cell interference. Furthermore, there have been several studies to enhance the efficiency of NOMA in the literature [10–14].

The aforementioned two promising technologies collectively can be adopted for the wireless local area networks (WLANs) [15]. WLAN, which has a service range of tens of meters, is widely utilized in many ways. Due to the characteristics of the simple implementation and low cost hardware, WLAN devices, e.g., access points (APs) and stations (STAs), can be densely deployed without sophisticated cell planning. This aspect may increase the portion of overlapping cell regions and decrease the throughput of users. The main focus of this work is to enhance the throughput in this highly dense and overlapped WLAN environment, especially in multi-cell scenarios.

In this paper, we will provide the joint scheduling and power allocation algorithm, which is named heuristic iterative water-filling (H-IWF), using non-orthogonal multiple access scheme in densely deployed multi-cell WLANs. Smart antenna technology, which enables spatial reuse in the wireless communication system, is adopted while considering the interference from other beams and other cells at the same time.

The major challenges associated with full-scale utilization of the very limited frequency resource and a novel methodology involving efficient power allocation, scheduling, and beamforming are presented, discussed, and verified. The joint optimization to find the feasible solution based on the iterative procedure confirms that the proposed method, which conforms to 802.11ax, can be used for stable and resource-efficient wireless link connections among future WLAN and 5G-based IoT (Internet of Things) devices. The compelling system-level simulation results further ascertain the feasibility of the proposed mmWave wireless solution for various IoT applications.

## 2. System Model and Problem Formulation

### 2.1. System Model

In the case of multi-cell WLAN scenarios, there is a set of cells  $\mathbb{G} = \{g_1, g_2, \dots, g_L\}$ . A cell  $g_l$  contains an AP and  $n_l$  users. An AP consists of multiple directional beams. Furthermore, a schedule set for the cell  $g$  is defined as  $\mathbb{S}^g = \{S_1^g, S_2^g, \dots, S_N^g\}$ , where a schedule includes two users for a single beam in a time slot, which is presented as  $S_i^g = \{u_{i,1}^g, u_{i,2}^g\}$ . When more than two users are allocated a schedule, finding a rate-region can be highly time consuming due to the complex calculation of multiple variables for optimization. Even if more than two users can be supported, two user scheduling is experimentally proven to be the most cost-efficient scheduling compared to other numbers of users in a schedule [16]. Thus, we assume the number of users in a schedule is two for a single beam in this scenario.

When we consider a schedule  $S_i^g$  that is scheduled by beam  $b$  with power  $p_b^g$  in the cell  $g$ , the power allocated to two users in the schedule is expressed as Equation (1):

$$\begin{aligned} p(u_{i,1}^g) &= \alpha p_b^g \\ p(u_{i,2}^g) &= (1 - \alpha) p_b^g \end{aligned} \quad (1)$$

where  $\alpha$  is the proportion of the beam power allocated to  $u_{i,1}^g$ .  $\mathbf{w}(u_{i,1}^g)$  is the interfering signal from the other beams and from other APs, and  $n(u_{i,1}^g)$  is additive white Gaussian noise at  $u_{i,1}^g$ . Then, the received signals of the users scheduled to beam  $b$  in a cell  $g$  are described as Equation (2):

$$\begin{aligned} r_{u_{i,1}^g} &= h_{b,u_{i,1}^g} S_i^g + \mathbf{w}(u_{i,1}^g) + n(u_{i,1}^g) \\ r_{u_{i,2}^g} &= h_{b,u_{i,2}^g} S_i^g + \mathbf{w}(u_{i,2}^g) + n(u_{i,2}^g) \end{aligned} \quad (2)$$

where  $h_{b,u_{i,1}^g}$  is the channel gain between an AP of cell  $g$  and node  $u_{i,1}^g$ , and  $\mathbf{w}(u_{i,1}^g)$  and  $n(u_{i,1}^g)$  are interference and white Gaussian noise with variance  $\sigma^2$  for node  $u_{i,1}^g$ , respectively.

We assume the user  $u_{i,1}^g$  is closer to the direction of beam  $b$  of an AP in the cell  $g$  than  $u_{i,2}^g$  and  $u_{i,1}^g$  can completely decode and cancel the packets for  $u_{i,2}^g$  because the power allocated to  $u_{i,2}^g$  is larger than the power allocated to  $u_{i,1}^g$ . When we consider collected interference at users  $u_{i,1}^g, u_{i,2}^g$  in AP  $g$  from the other APs as  $I_{u_{i,1}^g}^m, I_{u_{i,2}^g}^m$  and the intra-cell interference at the users, which is allocated to beam  $b$  as  $I_{b,u_{i,1}^g}, I_{b,u_{i,2}^g}$ , then we can obtain the throughput of users as Equations (3) and (4):

$$\begin{aligned}
C_{u_{i,1}^g}(\alpha, \mathbf{p}_g) &= W \log_2 \left( 1 + \frac{p(u_{i,1}^g) h_{b,u_{i,1}^g}}{I_{b,u_{i,1}^g} + I_{u_{i,1}^g}^m + \sigma^2} \right) \\
&= W \log_2 \left( 1 + \frac{\alpha p_b^g h_{b,u_{i,1}^g}}{\sum_{a \in \mathbb{B}_g, a \neq b} p_a h_{a,u_{i,1}^g} + \sum_{g_l \in \mathbb{G}, g_l \neq g} \sum_{b \in \mathbb{B}_{g_l}} p_b^{g_l} h_{b,u_{i,1}^g} + \sigma^2} \right)
\end{aligned} \quad (3)$$

$$\begin{aligned}
C_{u_{i,2}^g}(\alpha, \mathbf{p}_g) &= W \log_2 \left( 1 + \frac{p(u_{i,2}^g) h_{b,u_{i,2}^g}}{p(u_{i,1}^g) h_{b,u_{i,2}^g} + I_{b,u_{i,2}^g} + I_{u_{i,2}^g}^m + \sigma^2} \right) \\
&= W \log_2 \left( 1 + \frac{(1-\alpha) p_b^g h_{b,u_{i,2}^g}}{\alpha p_b^g h_{b,u_{i,2}^g} + \sum_{a \in \mathbb{B}_g, a \neq b} p_a h_{a,u_{i,2}^g} + \sum_{g_l \in \mathbb{G}, g_l \neq g} \sum_{b \in \mathbb{B}_{g_l}} p_b^{g_l} h_{b,u_{i,1}^g} + \sigma^2} \right)
\end{aligned} \quad (4)$$

where  $\mathbb{B}_g$  is the set of beams in a cell  $g$ ,  $\mathbf{p}_g$  is the beam power allocation vector for the beams in a cell  $g$ , and  $W$  is the bandwidth of the channel.

Now, we define the normalized throughput for the schedule  $S_i^g$  as:

$$C_i^g(\alpha, \mathbf{p}_g) = \frac{C_{u_{i,1}^g}(\alpha, \mathbf{p}_g)}{C_{u_{i,1}^g}(1, \mathbf{p}_g)} + \frac{C_{u_{i,2}^g}(\alpha, \mathbf{p}_g)}{C_{u_{i,2}^g}(0, \mathbf{p}_g)} \quad (5)$$

Here, both  $C_{u_{i,1}^g}(1, \mathbf{p}_g)$  and  $C_{u_{i,2}^g}(0, \mathbf{p}_g)$  represent the throughput of users  $u_{i,1}^g$  and  $u_{i,2}^g$  when all the beam power of cell  $g$ ,  $p_b^g$  is entirely allocated to those users, respectively. This normalized throughput measures the sum of rationality of the throughput of users when NOMA is applied compared to the throughput of users when NOMA is not applied, which evaluates the effectiveness of the NOMA scheme. Now, the optimal value of  $\alpha$  that maximizes the normalized throughput can be easily obtained by the value of  $\alpha$ , which makes the derivatives of Equation (5) equal to zero, because normalized the throughput in Equation (5) is a concave function.

$$\alpha_i^{g*} = \frac{h_{b,u_{i,1}^g} I_{u_{i,2}^g}^{mn} C_{u_{i,1}^g}(1, \mathbf{p}_g) - h_{b,u_{i,2}^g} I_{u_{i,1}^g}^{mn} C_{u_{i,2}^g}(0, \mathbf{p}_g)}{p_b^g h_{b,u_{i,1}^g} h_{b,u_{i,2}^g} (C_{u_{i,1}^g}(1, \mathbf{p}_g) - C_{u_{i,2}^g}(0, \mathbf{p}_g))} \quad (6)$$

where  $I_{u_{i,1}^g}^{mn} = I_{b,u_{i,1}^g} + I_{u_{i,1}^g}^m + \sigma^2$  means the interference plus noise power at user  $u_{i,1}^g$ , which is measured by the cumulative sum of interference from other beams in a single cell, interference from the other cells, and the noise power.

Finally, we can derive the explicit solution form of the maximum normalized capacity of the schedule  $S_i^g$  as the following Equation (7) using the optimal  $\alpha$  value as depicted in Equation (6).

$$\begin{aligned}
C_i^{g*}(\alpha, \mathbf{p}_g) &= C_i(\alpha_i^{g*}, \mathbf{p}_g) = \frac{W}{C_{u_{i,1}^g}(1, \mathbf{p}_g)} \log_2 \left( \frac{(h_{b,u_{i,1}^g} I_{u_{i,2}^g}^{mn} - h_{b,u_{i,2}^g} I_{u_{i,1}^g}^{mn}) C_{u_{i,2}^g}(0, \mathbf{p}_g)}{h_{b,u_{i,2}^g} I_{u_{i,1}^g}^{mn} (C_{u_{i,1}^g}(1, \mathbf{p}_g) - C_{u_{i,2}^g}(0, \mathbf{p}_g))} \right) \\
&+ \frac{W}{C_{u_{i,2}^g}(0, \mathbf{p}_g)} \log_2 \left( \frac{h_{b,u_{i,1}^g} (h_{b,u_{i,2}^g} p_b^g + I_{u_{i,2}^g}^{mn}) (C_{u_{i,1}^g}(1, \mathbf{p}_g) - C_{u_{i,2}^g}(0, \mathbf{p}_g))}{(h_{b,u_{i,1}^g} I_{u_{i,2}^g}^{mn} - h_{b,u_{i,2}^g} I_{u_{i,1}^g}^{mn}) C_{u_{i,1}^g}(1, \mathbf{p}_g)} \right)
\end{aligned} \quad (7)$$

## 2.2. Problem Formulation

In this section, an optimization problem that maximize the fairness among schedules considering users' average throughput is presented. The proportional fairness (PF) scheduler for NOMA maximizes  $\sum_{S_i^g \in \mathbb{S}_g} \log \left( \overline{R}(u_{i,1}^g; t) + \overline{R}(u_{i,2}^g; t) \right)$  where  $\mathbb{S}_g$  is defined as a set of schedules and  $\overline{R}(k; t)$  is the average throughput of user  $k$  at time  $t$  [17]. Then, we can define the average throughput of user  $k$  and the instant throughput of the user at time  $t$  as  $r(k; t)$ . When the averaging time period is  $\tau_c$ , the averaged throughput of user  $k$  can be recursively derived as Equation (8).

$$\overline{R}(k; t+1) = (1 - \tau_c) \overline{R}(k; t) + \tau_c r(k; t) \quad (8)$$

where:

$$r(k; t) = \begin{cases} C_k(\alpha_i^{g*}, \mathbf{p}_g) & k \in S_i^g \\ 0 & k \notin S_i^g \end{cases} \quad (9)$$

To perform the proportional fairness algorithm among users in the cells [17], we derive the objective function  $f(\mathbf{p}, \mathbf{e})$ , which is proportional to the instant normalized throughput and inversely proportional to the average user throughput of the users in a schedule. Then, we build an optimization problem that maximizes the sum of user throughput as Equation (11):

$$\begin{aligned} \max_{\mathbf{p}, \mathbf{e}} \quad & \sum_{g \in \mathbb{G}} \sum_{S_i \in \mathbb{S}_g} \sum_{b \in \mathbb{B}_g} e_{S_i, b}^g \left[ \frac{C_{u_{i,1}^g}(\alpha_i^{g*}, p_b^g) + C_{u_{i,2}^g}(\alpha_i^{g*}, p_b^g)}{\overline{R}(u_{i,1}^g) + \overline{R}(u_{i,2}^g)} \right] \\ \text{s.t.} \quad & p_b^g \geq 0, \sum_{b \in \mathbb{B}_g} p_b^g = P_{\max}, \\ & e_{S_i, b}^g \in \{0, 1\}, \sum_{S_i \in \mathbb{S}} e_{S_i, b}^g \leq 1, \forall S_i \in \mathbb{S}, \forall b \in \mathbb{B}_g \end{aligned} \quad (10)$$

Here,  $P_{\max}$  is the maximum power budget of an AP,  $p_b^g$  is the allocated power of beam  $b$  in a cell  $g$ , and  $e_{S_i, b}^g$  is the scheduling indicator, which is equal to one if a schedule  $S_i$  in a cell  $g$  is selected by beam  $b$ , otherwise zero.

## 3. Joint Scheduling and Power Allocation with NOMA

### 3.1. Optimality Conditions and Approximations

To solve the optimization problem specified in (11), we investigate the first order optimality conditions (12)–(17). The Lagrangian of the original optimization problem is derived as follows.

$$L(\mathbf{p}, \mathbf{e}, \lambda, \mu) \triangleq f(\mathbf{p}, \mathbf{e}) + \sum_{g \in \mathbb{G}} \lambda_g \left( P_{\max} - \sum_{b \in \mathbb{B}_g} p_b^g \right) + \sum_{g \in \mathbb{G}} \sum_{b \in \mathbb{B}_g} \mu_{g,b} \left( 1 - \sum_{S_i \in \mathbb{S}} e_{S_i, b}^g \right) \quad (11)$$

where  $\lambda \triangleq (\lambda_1, \dots, \lambda_G)^T$  and  $\mu \triangleq \text{vec}\{\mu_1, \dots, \mu_G\}$  with  $\mu_g \triangleq (\mu_{g,1}, \dots, \mu_{g,B_g})^T$  are non-negative Lagrangian multipliers.

$$p_b^g \left( \frac{\partial f(\mathbf{p}, \mathbf{e})}{\partial p_b^g} - \lambda \right) = 0 \quad (12)$$

$$e_{S_i, b}^g \left( \frac{\partial f(\mathbf{p}, \mathbf{e})}{\partial e_{S_i, b}^g} - \mu_b \right) = 0 \quad (13)$$

$$\lambda \left( P_{\max} - \sum_{b \in \mathbb{B}_g} p_b^g \right) = 0 \quad (14)$$

$$\mu_b \left( 1 - \sum_{S_i \in \mathbb{S}} e_{S_i, b}^g \right) = 0 \quad (15)$$

where:

$$\frac{\partial f(\mathbf{p}, \mathbf{b})}{\partial p_b^g} = \frac{e_{S_i, b}^g}{\ln 2 \left( \overline{R(u_{i,1}^g)} + \overline{R(u_{i,2}^g)} \right)} \cdot \left( \frac{\alpha_i^{g*} h_{b, u_{i,1}^g}}{I_{u_{i,1}^g}^{mn} + \alpha_i^{g*} p_b^g h_{b, u_{i,1}^g}} + \frac{I_{u_{i,2}^g}^{mn} (1 - \alpha_i^{g*}) h_{b, u_{i,2}^g}}{(I_{u_{i,2}^g}^{mn} + p_b^g h_{b, u_{i,2}^g}) (I_{u_{i,2}^g}^{mn} + \alpha_i^{g*} p_b^g h_{b, u_{i,2}^g})} \right) \quad (16)$$

$$\frac{\partial f(\mathbf{p}, \mathbf{b})}{\partial e_{S_i, b}^g} = \frac{C_{u_{i,1}^g}(\alpha_i^{g*}, p_g) + C_{u_{i,2}^g}(\alpha_i^{g*}, p_g)}{\overline{R(u_{i,1}^g)} + \overline{R(u_{i,2}^g)}} \quad (17)$$

To maximize the objective function  $f(\mathbf{p}_g, \mathbf{b})$ , by substituting (17) to (13), we can derive a set of schedules that maximizes the objective function. As a result, beam  $b$  of a cell  $g$  should be allocated to schedule  $S_i^g$  by the following Equation (18).

$$S_b^{g,opt} = \arg \max_{S_i^g \in \mathbb{S}_g} \left( \frac{C_{u_{i,1}^g}(\alpha_i^{g*}, p_b) + C_{u_{i,2}^g}(\alpha_i^{g*}, p_b)}{\overline{R(u_{i,1}^g)} + \overline{R(u_{i,2}^g)}} \right) \quad (18)$$

The power constrained condition (12) can be solved when the derivative of objective function  $\frac{\partial f(\mathbf{p}, \mathbf{b})}{\partial e_{S_i, b}^g}$  is substituted by Equation (16). However, it is not possible to obtain an explicit and feasible solution with respect to  $p_b^g$ . Here, we suggest an approximation to this beam power allocation. Since the first user in a schedule, denoted as  $u_{i,1}^g$ , contributes further to the scheduler, i.e.,  $C_{u_{i,1}^g}(\alpha_i^{g*}, p_b^g) > C_{u_{i,2}^g}(\alpha_i^{g*}, p_b^g)$  and  $\overline{R(u_{i,1}^g)} > \overline{R(u_{i,2}^g)}$ , the objective function for the beam power allocation may consider the first user only. Then, Equation (16) can be reduced as follows.

$$\begin{aligned} \frac{\partial f(\mathbf{p}_g, \mathbf{b})}{\partial p_b^g} \approx & \frac{1}{\ln 2 \cdot \overline{R(u_{i,1}^g)}} \times \left( \frac{e_{S_i, b}^g h_{b, u_{i,1}^g}}{p_b^g h_{b, u_{i,1}^g} + I_{u_{i,1}^g}^{mn}} - \sum_{a \in \mathbb{B}_g, a \neq b} \sum_{S_m^g \in \mathbb{S}_g} \frac{e_{S_m, a}^g h_{b, u_{m,1}^g}}{\sigma^2 + \sum_{g_l \in \mathbb{G}} \sum_{b \in \mathbb{B}_l} p_b^{g_l} h_{b, u_{i,1}^g}} \cdot \frac{p_a^g h_{a, u_{m,1}^g}}{I_{u_{i,1}^g}^{mn}} \right. \\ & \left. - \sum_{l \in \mathbb{G}, l \neq g} \sum_{a \in \mathbb{B}_l} \sum_{S_m^l \in \mathbb{S}_l} \frac{e_{S_m, a}^l h_{b, u_{m,1}^l}}{\sigma^2 + \sum_{g_l \in \mathbb{G}} \sum_{b \in \mathbb{B}_l} p_b^{g_l} h_{b, u_{i,1}^l}} \cdot \frac{p_a^l h_{a, u_{m,1}^l}}{I_{u_{i,1}^l}^{mn}} \right) \end{aligned} \quad (19)$$

Finally, the optimal power allocation  $p_b^{g*}$  as the solution of (12) can be calculated by using (19).

$$p_b^{g*} = \left[ \frac{e_{S_i, b}^g}{\lambda \ln 2 + t_b + t_g} - \frac{I_{u_{i,1}^g}^{mn}}{h_{b, u_{i,1}^g}} \right]^+ \quad (20)$$

The solution of the power allocation problem contains taxation terms  $t_b$  and  $t_g$ .  $t_b$  measures the summation of the total received power from other beams that are not allocated to users in this schedule, and  $t_g$  means the cumulative power of beams from other cells. These two taxation terms are defined as Equations (21) and (22).

$$t_b \triangleq \sum_{a \in \mathbb{B}, a \neq b} \sum_{m \in \mathbb{K}} \frac{b_{m,a} h_{b,m}}{\sigma^2 + \sum_{j \in \mathbb{B}} p_j h_{j,m}} \cdot \frac{p_a h_{a,m}}{\sigma^2 + \sum_{c \in \mathbb{B}, c \neq a} p_c h_{c,m}} \quad (21)$$

$$t_g \triangleq \sum_{l \in \mathbb{G}, l \neq g} \sum_{a \in \mathbb{B}_l} \sum_{S_m^l \in \mathbb{S}_l} \frac{e_{S_m^l, a}^l h_{b, u_{m,1}^l}}{\sigma^2 + \sum_{g_l \in \mathbb{G}} \sum_{b \in \mathbb{B}_{g_l}} p_b^{g_l} h_{b, u_{i,1}^{g_l}}} \cdot \frac{p_a^l h_{a, u_{m,1}^l}}{I_{u_{i,1}^l}^{mn}} \quad (22)$$

Overall, the beam power allocation constraint can be obtained by substituting (10) with (20) as Equation (23).

$$P_{\max} = \sum_{b \in \mathbb{B}_g} \left[ \frac{e_{S_i, b}^g}{\lambda \ln 2 + t_b + t_g} - \frac{I_{u_{i,1}^l}^{mn}}{h_{b, u_{i,1}^g}} \right]^+ \quad (23)$$

### 3.2. Heuristic Iterative Water-Filling

For this subsection, we present the overall joint scheduling strategy and power allocation for multi-cell environments. The complexity of resource allocation is significantly considerable because of the recursive calculation between power allocation and the scheduling process. Therefore, we decompose the scheduling process into the beam allocation process and beam power allocation process so that suboptimal solutions can be found in real time. In our proposed algorithm, beam allocation and power allocation are performed sequentially. The detailed procedure of the proposed iterative water-filling algorithm is given as follows.

When using Algorithm 1, the complexity of the algorithm is  $O(N^2 \times G)$ . Since there is a number of users, it is necessary to reduce the complexity of the algorithm. However, this system should consider all users and build a schedule that contains two users. It is hard to develop a suboptimal algorithm that achieves both throughput and fairness compared to the exhaustive search of all schedules. Here, we propose the grouping algorithm that has reduced complexity compared to the former algorithm. In this grouping algorithm, the users are divided into two groups, which are near users  $N_n$  and far users  $N_f$ , and the users selected in a schedule should be chosen from two cells. For example, users in a schedule  $S_i$  should be distinguished into two sets of users,  $u_{i,1}^g \in N_n$ ,  $u_{i,2}^g \in N_f$ . For this rule, the complexity of the algorithm is reduced from  $O(N^2 \times G)$  to  $O(N \log N \times G)$ . The performance of the grouping algorithm will be numerically discussed at the end of the performance evaluation sections.

**Algorithm 1** Heuristic iterative water-filling algorithm for multi-cell WLAN**(1) Initialization**

Initialize  $\mathbf{p} = \text{vec}\{\mathbf{p}_{g_1}, \dots, \mathbf{p}_{g_L}\}$  where  $\mathbf{p}_{g_i} = (p_1^{g_i}, \dots, p_B^{g_i})^T$  where  $p_b^{g_i} = \frac{P_{\max}}{B}$ .

**Repeat****(2) Beam allocation**

Allocate beam  $\mathbf{e}$  based on initialized  $\mathbf{p}^*$  according to (10)

**for**  $g_i = g_1$  to  $g_L$  **do**

**for**  $b = 1$  to  $B$  **do**

        Select schedule  $S^{b,opt}$  according to (18)

$$S_b^{g_i,opt} = \arg \max_{S_i^{g_i} \in \mathcal{S}_{g_i}} \left( \frac{C_{u_{i,1}^{g_i}}(\alpha_i^{g_i*}, p_b) + C_{u_{i,2}^{g_i}}(\alpha_i^{g_i*}, p_b)}{R(u_{i,1}^{g_i}) + R(u_{i,2}^{g_i})} \right)$$

    Allocate beam  $b$  to schedule  $S_b^{g_i,opt}$

$$e_{S_b^{g_i,opt}, b}^{g_i} = 1, e_{S_k^{g_i}, b}^{g_i} = 0 \quad \forall S_k^{g_i} \neq S_b^{g_i,opt}$$

**end**

**end**

**(3) Power allocation**

Allocate beam power  $\mathbf{p}$  based on allocated  $\mathbf{e}$

Find  $\lambda$  according to (23) by using the bisection method

**for**  $g_i = g_1$  to  $g_L$  **do**

**for**  $b = 1$  to  $B$  **do**

        Compute  $p_b^{g_i}$  according to (20)

**end**

**end**

**Until**

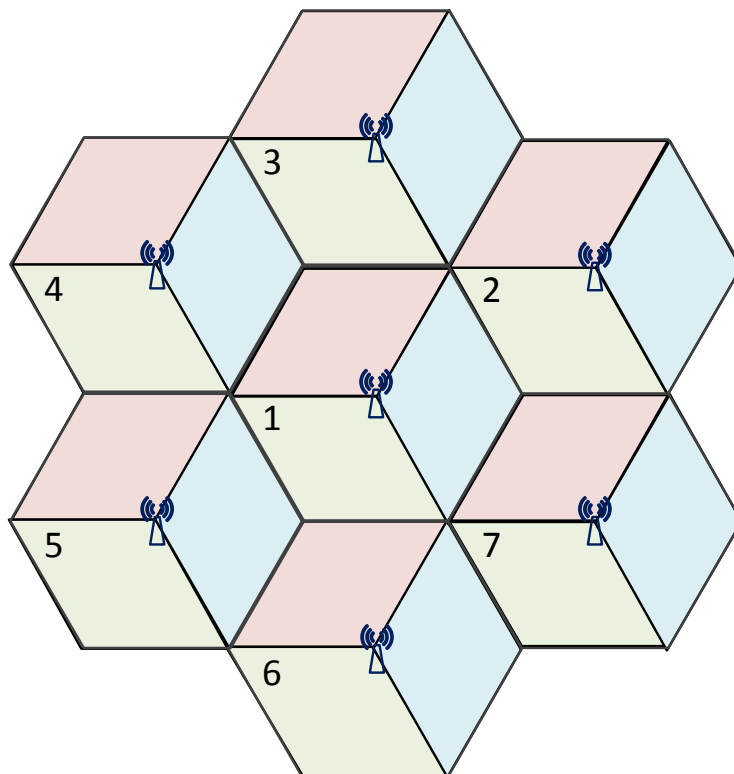
**4. Performance Evaluation***4.1. Parameter for System Level Performance Evaluation*

To evaluate the proposed scheduling scheme, we performed intensive simulations at the system level by using the MATLAB simulator. All the simulation parameters were chosen based on the practical evaluation models in the specification documents and the contribution documents for standardization of IEEE 802.11ax [15,18]. A seven-cell structure was considered in the simulations. Each cell contained an AP and users. A maximum of 30 users were uniformly distributed in a hexagonally-shaped cell, and we defined the AP at the center of the system structure as the center AP. Each cell was assumed to cover the radius of a 10 m area. Downlink traffic with infinite backlog was assumed. The beam width of each sector beam was  $120^\circ$ , and the number of beams was  $B = 3$ . Furthermore, the 3 dB beamwidth  $\theta_{3dB}$  of each beam was  $\theta_{3dB} = 70^\circ$  for the three sector antenna [19]. The maximum attenuation  $A_m$  and the antenna gain  $G_A$  were 20 dB and 14 dBi. User throughput was averaged over 1024 ms when the scheduling was performed for each 1 ms. The distance-dependent path loss exponent was set to 3.5 [20]. The noise spectral density was  $-174$  dBm/Hz. Table 1 shows the simulation parameters that we used based on the IEEE 802.11 ax specifications, which was devised for dense network small cell indoor scenarios [18].

**Table 1.** Simulation parameters for multi-cell WLANs.

Parameter	Value
Cell radius	10 m
Distance between two cells	34.6 m/17.3 m
Maximum number of users in a cell	30
Number of beams in a cell	3
Carrier frequency	2.4 GHz
Channel bandwidth	20 MHz
Noise spectral density	−174 dBm/Hz
Scheduling interval	1 ms
Throughput averaging interval ( $\tau_c$ )	1024 ms
Maximum transmittable power of AP ( $P_{max}$ )	20 dBm
Path-loss (dB) [20]	$31.5 + 35 \log_{10}(d)$

The proposed algorithm was compared to the conventional scheme, in which the beam power was same, i.e.,  $p_b^g = 17$  dBm. The NOMA-based scheduling scheme allocates power to users in a schedule based on (6), and the OMA-based scheduling scheme distributes each resource block as a portion of  $\alpha$ , which was selected above. Here, the shape of the cell was hexagonal with three  $120^\circ$  beams, and the center cell was denoted as the cell that was located at the center of the example network topology. In other words, the other six cells surrounded the center cell, which is shown in Figure 1.

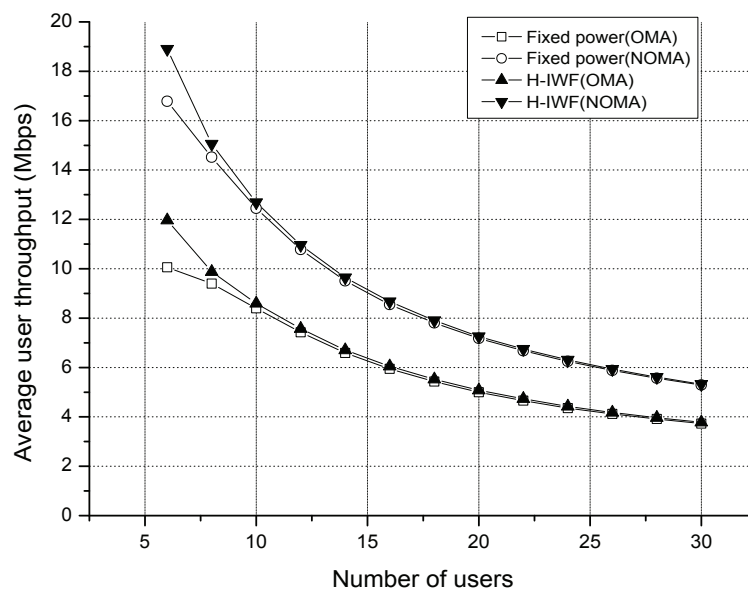
**Figure 1.** Topology for multi-cell transmission.

#### 4.2. Simulation Results and Discussions

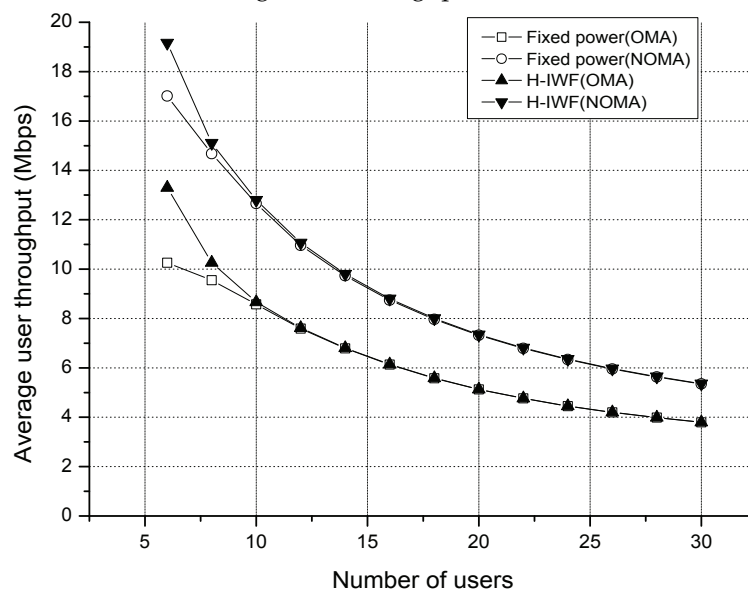
Figure 2 shows the average user throughput, which was measured for the multi-cell WLANs based on the IEEE 802.11 ax specifications when the inter-cell distance equaled 34.6 m. Figure 2a shows the average user throughput, which was measured for all seven APs. It shows that even in the multi-cell environment when inter-cell interference existed, the NOMA-based resource allocation achieved about a 50% gain compared to the OMA-based resource allocation. Furthermore, the proposed iterative



water-filling algorithm could achieve throughput gain regardless of the number of users. The gain of water-filling was relatively larger in the case of a small number of users, because the variation of the channel gain among the users was higher when the number of users was small. Figure 2b shows the average throughput of the center cell. Since the center cell experienced the most severe inter-cell interference compared to other cells, the average throughput was smaller than that all cells, which is shown in Figure 2a. However, it shows that the proposed scheme still worked even in the situation in which much interference existed.



(a) Average user throughput for all APs

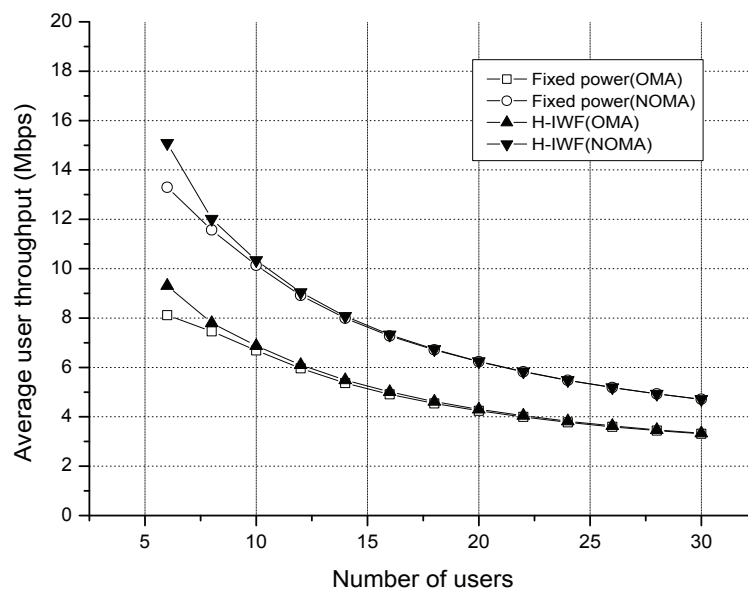


(b) Average user throughput for the AP of the center cell

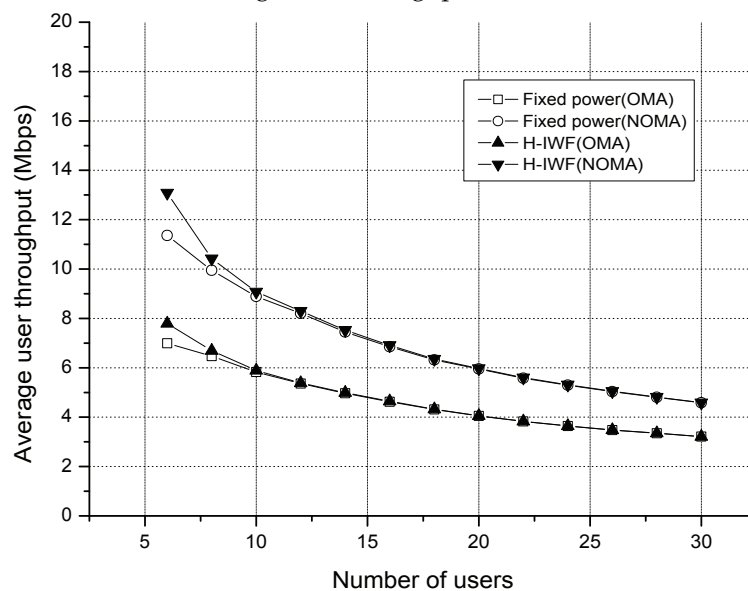
**Figure 2.** Average throughput vs. the number of users when the inter-cell distance equals 34.6 m. H-IWF, heuristic iterative water-filling.

Figure 3 presents the case of a severely dense environment in which the inter-cell distance was reduced by half compared to the case of Figure 2. Since the cells were closer compared to the former case, the portion of overlapped region increased, and the interference from other APs also increased. As a result, the overall average user throughput shown in Figure 3a decreased. The AP and users in

the center cell suffered more severely from throughput degradation as shown in Figure 3b. Compared to the result averaged for all AP, the degradation level was 7.1%, while it was 1.7% in the results of the inter-cell distance of 34.6 m. Considering the practical WLAN deployment, this kind of highly dense scenario is inevitable in real environments. Thus, it needs to be addressed that the proposed scheme can work in highly severe cases. Aside from the unavoidable throughput decrease in densely deployed environments, we observed that the proposed algorithm could achieve 50% of user throughput gain on average.



(a) Average user throughput for all APs



(b) Average user throughput for the AP of the center cell

Figure 3. Average throughput vs. the number of users when inter-cell distance equals 17.3 m.

## 5. Conclusions

The major challenge associated with densely deployed wireless networks and the novel optimization methodology involving efficient scheduling and beam power allocations were presented, discussed, and verified, while taking into account NOMA and smart antenna-based beamforming technology in multi-cell environments. Empirical data from intensive simulations at the system level

confirmed that the proposed algorithm could be used for stable wireless link connections in IEEE 802.11ax. The compelling results further ascertained the feasibility of the proposed iterative scheme for various applications.

**Author Contributions:** K.S. modeled the system, as well as validated it with simulation and performed the original draft preparation. O.J. contributed to the review and editing, determined the topology, performed the data analysis, and provided resources and supervision. All authors read and agreed to the published version of the manuscript.

**Funding:** This research received no external funding.

**Acknowledgments:** This work was supported by the National Research Foundation of Korea(NRF) Grant No. NRF-2018R1C1B5043899.

**Conflicts of Interest:** The authors declare no conflict of interest.

## References

- Otao, N.; Kishiyama, Y.; Higuchi, K. Performance of non-orthogonal access with SIC in cellular downlink using proportional fair-based resource allocation. In Proceedings of the International Symposium on Wireless Communication Systems (ISWCS) 2012, Paris, France, 28–31 August 2012; pp. 476–480.
- Takeda, T.; Higuchi, K. Enhanced User Fairness Using Non-Orthogonal Access with SIC in Cellular Uplink. In Proceedings of the IEEE Vehicular Technology Conference (VTC Fall) 2011, San Francisco, CA, USA, 5–8 September 2011.
- Jo, O.; Hong, W.; Choi, S.; Chag, S.; Kweon, C.; Oh, J.; Cheun, K. Holistic design considerations for environmentally adaptive 60 GHz beamforming technology. *IEEE Commun. Mag.* **2014**, *52*, 30–38. [\[CrossRef\]](#)
- Jo, O.; Yoon, J. Spatial reuse algorithm using interference graph in millimeter wave beamforming systems. *Etri J.* **2017**, *39*, 255–263. [\[CrossRef\]](#)
- Zhao, N.; Li, D.; Liu, M.; Cao, Y.; Chen, Y.; Ding, Z.; Wang, X. Secure transmission via joint precoding optimization for downlink MISO NOMA. *IEEE Trans. Veh. Technol.* **2019**, *68*, 7603–7615. [\[CrossRef\]](#)
- Felici-Castell, S.; Navarro, A.; Pérez-Solano, J.; Segura-García, J.; García-Pineda, M. Practical considerations in the implementation of collaborative beamforming on wireless sensor networks. *Sensors* **2017**, *17*, 237. [\[CrossRef\]](#) [\[PubMed\]](#)
- Navarro-Camba, A.; Felici-Castell, S.; Segura-García, J.; García-Pineda, M.; Pérez-Solano, J. Feasibility of a Stochastic Collaborative Beamforming for Long Range Communications in Wireless Sensor Networks. *Electronics* **2018**, *7*, 417. [\[CrossRef\]](#)
- Jo, O.; Shin, K. Joint scheduling and power allocation using non-orthogonal multiple access in directional beam-based WLAN systems. *IEEE Wirel. Commun. Lett.* **2017**, *6*, 482–485.
- Zhang, J.; Andrews, J. Adaptive Spatial Intercell Interference Cancellation in Multicell Wireless Networks. *IEEE J. Sel. Areas Commun.* **2010**, *28*, 1455–1468. [\[CrossRef\]](#)
- Wu, Y.; Zhang, C.; Ni, K.; Qian, L.; Huang, L.; Zhu, W. Optimal Resource Allocation for Uplink Data Collection in Nonorthogonal Multiple Access Networks. *Sensors* **2018**, *18*, 2542. [\[CrossRef\]](#) [\[PubMed\]](#)
- Selvaprabhu, P.; Chinnadurai, S.; Sarker, M.; Lee, M. Joint Interference Alignment and Power Allocation for K-User Multicell MIMO Channel through Staggered Antenna Switching. *Sensors* **2018**, *18*, 380. [\[CrossRef\]](#) [\[PubMed\]](#)
- Ahn, J.; Kim, Y.; Kim, R. A Novel WLAN Vehicle-To-Anything (V2X) Channel Access Scheme for IEEE 802.11p-Based Next-Generation Connected Car Networks. *Appl. Sci.* **2018**, *8*, 2112. [\[CrossRef\]](#)
- Wang, Z.; Yu, H.; Wang, D. Channel and Bit Adaptive Power Control Strategy for Uplink NOMA VLC Systems. *Appl. Sci.* **2019**, *9*, 220. [\[CrossRef\]](#)
- Ding, Z.; Fan, P.; Poor, V. Random beamforming in millimeter-wave NOMA networks. *IEEE Access* **2017**, *5*, 7667–7681. [\[CrossRef\]](#)
- IEEE 802.11-2012. Part 11: Wireless LAN Medium Access Control (MAC) and Physical Layer (PHY) Specifications; IEEE: Piscataway, NJ, USA, 2012.
- Vanka, S.; Srinivasa, S.; Gong, Z.; Vizi, P.; Stamatiou, K.; Haenggi, M. Superposition coding strategies: Design and experimental evaluation. *IEEE Trans. Wirel. Commun.* **2012**, *11*, 2628–2639. [\[CrossRef\]](#)
- Kelly, F.; Maulloo, A.; Tan, D. Rate control for communication networks: shadow prices, proportional fairness and stability. *J. Oper. Res. Soc.* **1998**, *49*, 237–252. [\[CrossRef\]](#)

18. *IEEE Standard 802.11-14/0980r1, TGax Simulation Scenarios*; IEEE: Piscataway, NJ, USA, 2015.
19. ETSI. *Spatial Channel Model for MIMO Simulations*; Tech. Rep. 125.996 V11.0.0; ETSI: Darmstadt, Germany, 2012.
20. Baum, D.; Hansen, J.; Salo, J. An interim channel model for beyond-3G systems: extending the 3GPP spatial channel model (SCM). In *Proceedings of the IEEE Vehicular Technology Conference (VTC Spring) 2005*, Stockholm, Sweden, 30 May–1 June 2005; pp. 3132–3136.



© 2020 by the authors. Licensee MDPI, Basel, Switzerland. This article is an open access article distributed under the terms and conditions of the Creative Commons Attribution (CC BY) license (<http://creativecommons.org/licenses/by/4.0/>).